Proc. Natl. Acad. Sci. USA
Vol. 95, pp. 15327–15332, December 1998
Biophysics

Cytologically normal cells from neoplastic cervical samples display extensive structural abnormalities on IR spectroscopy: Implications for tumor biology

MENASHI A. COHENFORD*† AND BASIL RIGAS‡§

*Digilab Division, Bio-Rad, Cambridge, MA 02139; and ‡Rockefeller University, New York, NY 10021

Communicated by William P. Jencks, Brandeis University, Waltham, MA, October 16, 1998 (received for review June 17, 1998)

ABSTRACT **Fourier-transform IR (FT-IR) spectra of pelleted exfoliated cervical cells from patients with cervical cancer or dysplasia differ from those from normal women. To study the origin of these spectral changes, we obtained the FT-IR spectra of individual cervical cells from normal, dysplastic, and malignant cervical samples. Ninety five percent of normal superficial and intermediate cells displayed two distinct spectral patterns designated A and B, and 5% displayed an intermediate pattern, suggesting extensive structural heterogeneity among these cells. Parabasal and endocervical cells showed pattern B spectra. The spectra of malignant, dysplastic, and other abnormal cells also were characterized. Analysis of FT-IR spectra of over 2,000 individual cells from 10 normal females, 7 females with dysplasia, and 5 females with squamous cell carcinoma revealed that the spectra of normal-appearing intermediate and superficial cells of the cervix from women with either dysplasia or cancer differed from those of normal women. Chemometric and classical spectroscopic analysis showed a continuum of changes paralleling the transition from normalcy to malignancy. These findings suggest that (*i*) the structural changes underlying the spectroscopic changes are involved in or are a product of cervical carcinogenesis and (*ii*) the neoplastic process may be more extensive than currently recognized with morphological criteria. This approach may be useful for the structural study of neoplasia and also may be of help in the diagnosis or classification of cervical disorders.**

Fourier-transform IR spectroscopy (FT-IR) is an emerging method for the study of cancer. We and others have observed that the FT-IR spectra of several human cancers—including colon, skin, and cervical cancer (1–5)—differ from those of their corresponding normal tissues. In cervical cancer, spectral abnormalities have been observed not only in malignant cervical scrapings but also in those with the premalignant condition cervical dysplasia. These findings suggest the occurrence of significant structural, chemical, or metabolic changes associated with cervical carcinogenesis, even at its early stages, and raise the possibility that IR spectroscopy may be useful in the diagnosis of cervical neoplasias.

The origin of the spectral changes associated with cervical neoplasia remains unknown. Published studies of exfoliated cervical cells (4–8) have examined pelleted cells, with each spectrum resulting from all cells and extracellular components in the path of the IR beam. Although it appears intuitive that the spectral abnormalities originate in the abnormal cells, proof of this has never been provided. Furthermore, it seems paradoxical that pellets of neoplastic samples (in which the dysplastic or malignant cells are often $<2\%$ of the total) generate grossly abnormal spectra.

Resolving these issues requires assessment of the contribution of the individual cellular and noncellular components to the spectra of cervical pellets. To this end, we have developed an approach to obtain FT-IR spectra from individual cells. By using this methodology, we have evaluated single cervical cells from normal, dysplastic, and malignant cervical samples. Here we present the results of our work, which indicate that in neoplastic cervical samples, cytologically normal cells exhibit extensive IR spectroscopic changes, implying significant structural changes.

MATERIALS AND METHODS

Cervical Specimens. We evaluated the cervical samples of 22 women: 10 normal, with no history of cervical pathology (average age 33 yr, range 26–41); 7 with dysplasia confirmed by subsequent biopsy (36 yr, range 28–55); and 5 with biopsy-proven cervical squamous cell carcinoma (45 yr, range 38–51). No patient was on oral contraceptives or had received chemo- or radiotherapy. The appropriate ethics committees approved the study, and all patients gave their consent.

Cervical scrapings were collected by using the standard brushing procedure. Exfoliated cells were released by shaking the brush in a solution (PreservCyt, CYTYC, Marlborough, MA) that preserved cellular integrity and lysed red blood cells. The cell suspension was processed in a Cytyc ThinPrep Processor, which filtered out mucus and debris and spread the cells uniformly on microscope slides.

FT-IR Microspectroscopy. FT-IR microspectroscopy was performed on unstained exfoliated cells, which were then photographed and their position recorded. Cells were fixed on a ZnS microscope slide. ZnS allowed viewing of the cells under a conventional and an IR microscope, was resistant to the Papanicolaou stains, and provided a suitable matrix for IR spectra acquisition. We used a Bio-Rad FT-IR UMA-500 microscope linked to an FTS165 spectrometer. Cells were selected at random; as the morphological features of unstained cells were barely detectable under low magnification, their selection was unbiased. The aperture was adjusted to within the cytoplasmic border of each cell; 700 spectra were co-added at a resolution of 8 cm^{-1}. A single-beam spectrum of the ZnS window served as the background reference of each spectrum. After spectroscopy, slides were stained with the Papanicolaou stain.

Chemometric Analysis. Commercial software (PLSplus, Galactic Industries, Salem, NH) was used for partial least squares. This analysis also evaluated visibly undetectable, subtle spectral differences. All spectra were normalized to a minimum and maximum absorbance value of 0.0 and 1.0, respectively. Normalization was confined to the region between 1,000 and 3,000 cm^{-1}—the region with most of the spectral changes in the abnormal cervical specimens. Chemometric analysis focused on the regions 1,200–1,000 cm^{-1} and 3,000–2,800 cm^{-1}; the region between 2,800 and 1,200 cm^{-1}

The publication costs of this article were defrayed in part by page charge payment. This article must therefore be hereby marked "*advertisement*" in accordance with 18 U.S.C. §1734 solely to indicate this fact.

Abbreviation: FT, Fourier transform.

†Present address: CYTYC Corporation, Boxborough, MA 01719.
§To whom reprint requests should be addressed at: Box 330, Rockefeller University, 1230 York Avenue, New York, NY 10021.

provided no significant information and was not analyzed. Calculation of F ratios and assignment of probability values to different spectra based on F ratio results were performed as described (9, 10). Spectra with F ratios corresponding to probability values >0.99 were flagged as outliers and not used for analysis. Ranks for different calibration spectra were selected on the basis of the Prediction Residual Error Sum of Squares (PRESS) and comparison of the PRESS values with all ranks before the PRESS value at the minimum. The first rank that fell below the cut-off probability level of 0.75 in the F test was the optimal rank for the analysis.

RESULTS

FT-IR Microspectroscopy of Normal Cervical Cells. Of the four main types of squamous cervical (superficial, intermediate, parabasal and basal), superficial, and intermediate cells represent the overwhelming majority in a conventional smear. Parabasal cells occur less frequently, and basal cells are exceedingly rare. Endocervical cells sometimes are seen. We obtained FT-IR spectra from all of these types of cells (Fig. 1).

The superficial and intermediate squamous epithelial cells yielded two main spectral patterns, designated A and B, and a less frequent pattern, intermediate between A and B ("mixed pattern"). Each of these patterns was virtually identical in these two cell types. Patterns A or B were observed in ≈90% of cervical cells (Table 1). Pattern A is characterized by a prominent band peaking at 1,027.20 ± 0.84 cm^{-1} (this and all subsequent values are mean ± SD, Table 2) and discrete bands at 1,080.43 ± 0.34

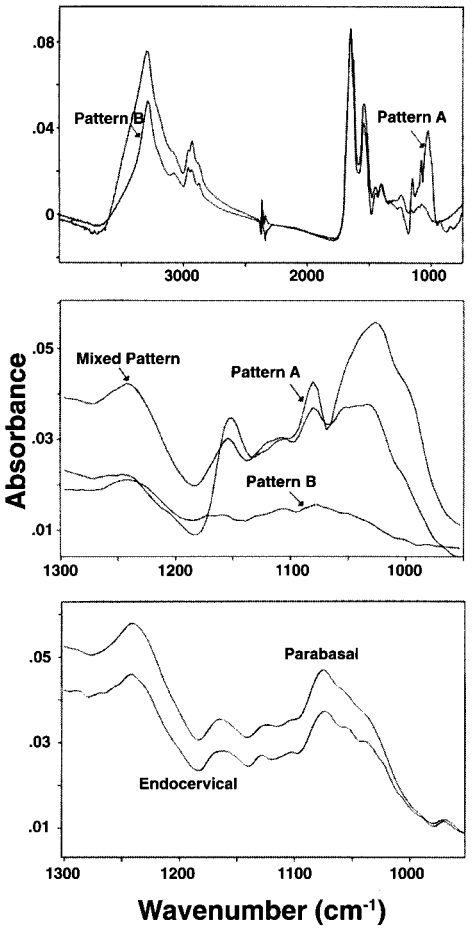

FIG. 1. IR spectra of normal cervical epithelial cells. The main spectral patterns (A and B) of superficial cells are shown in the region 900 cm^{-1}–4,000 cm^{-1} (*Top*) and in detail in the *Middle* (region 900–1,250 cm^{-1}), which also shows the mixed pattern. *Bottom,* the spectra of parabasal squamous and endocervical cells. Both belong to pattern B; the absence of the 1,026 cm^{-1} peak is characteristic.

Table 1. The frequency of IR spectral patterns in cervical smears

Sample	Cells, no. observed	Pattern A, %	Pattern B, %	Intermediate pattern, %	Poor quality, %
Normal (n = 10)					
1	105	29	58	7	6
2	100	44	38	18	3
3	100	47	43	4	6
4	100	31	59	7	3
5	101	1	81	2	16
6	98	25	63	3	9
7	100	51	34	4	11
8	100	81	15	0	4
9	100	94	3	3	0
10	100	20	72	4	4
Dysplasia (n = 7)					
1	104	23	67	2	8
2	99	3	82	6	8
3	103	3	91	1	5
4	84	12	67	10	12
5	99	40	47	2	11
6	102	55	39	2	4
7	101	9	86	3	2
Cancer (n = 5)					
1	100	37	54	4	5
2	100	9	88	1	2
3	98	38	55	4	3
4	94	7	82	2	9
5	99	56	40	2	2

There are no statistically significant differences between groups, except for the increased frequency of pattern B spectra in dysplastic samples, compared to normal samples (P = 0.05, Mann–Whitney U test).

cm^{-1}, 1,105.75 ± 2.11 cm^{-1} (identifiable in about 1/3 of the spectra), 1,153.38 ± 0.71 cm^{-1}, 1,242.25 ± 4.22 cm^{-1}, and two conspicuous peaks at 1,544.01 ± 1.68 cm^{-1} and 1,652.38 ± 0.48 cm^{-1}. Pattern B is characterized by a significant reduction in the amplitude of the 1,027 cm^{-1} band (which often is flattened), by bands at 1,079.16 ± 2.60 cm^{-1}, 1,114.41 ± 4.53 cm^{-1}, and 1,171.7 ± 6.43 cm^{-1}, by a band at 1,241.63 ± 3.23 cm^{-1} whose intensity is increased compared with that of pattern A, and by discrete bands at 1,544.51 ± 1.56 cm^{-1} and 1,653.58 ± 2.7 cm^{-1}. The position of peaks is not significantly different between the two patterns, except for the 1,105 cm^{-1} and the 1,153 cm^{-1} peaks, which in pattern B have been shifted to 1,114 cm^{-1} ($P < 0.001$) and 1,171 cm^{-1} ($P < 0.002$), respectively. The intermediate pattern was exhibited by about 5% of the cells. About 6% of cells yielded poor-quality spectra.

Glycogen, common in normal squamous epithelial cells of the cervix (3, 11), contributes significantly to these spectra. The spectrum of mammalian glycogen shows prominent bands at 1,026, 1,080, and 1,155 cm^{-1}, all readily seen in pattern A spectra (data not shown). To further evaluate glycogen's contribution to the spectra, cells were stained with either Lugol's reagent or periodic acid immediately after microspectroscopy. All cells exhibiting pattern A spectra stained positively for glycogen. No staining for glycogen was observed in any of the cells yielding typical pattern B spectra or those lacking the 1,026 cm^{-1} and 1,155 cm^{-1} spectral features. Cells yielding the intermediate pattern stained positive for glycogen, but their staining was less pronounced compared with cells exhibiting pattern A spectra. These findings further support the assignment of the 1,026 cm^{-1} and 1,155 cm^{-1} bands, at least partially, to glycogen.

The symmetric phosphate-stretching modes contribute to the 1,080 cm^{-1} band as well (1–3), and may originate from the phosphodiester groups of nucleic acids (12). The asymmetric phosphate-stretching modes contribute to the band at 1,244 cm^{-1}, which is not seen in the IR spectrum of glycogen. The bands at

1,652 cm^{-1} and 1,545 cm^{-1} represent amide I and amide II bands, respectively.

Parabasal cells yielded spectra similar to pattern B. The absence of the 1,026 cm^{-1} peak, suggesting a lack of glycogen, is consistent with both cytochemical findings and the notion that parabasal cells are less mature than superficial cells (11). Endocervical cells yielded spectra similar to pattern B. Because of their rarity, our study of endocervical and parabasal cells was not exhaustive.

FT-IR Microspectroscopy of Abnormal Cervical Cells. We assessed the FT-IR spectra of dysplastic and malignant cervical cells (Fig. 2) and also of koilocytes and anucleated cells; because of their scarcity, only a limited number of them were evaluated.

The spectra of dysplastic cells were characterized by reduced amplitude of the 1,026 cm^{-1} band, which is intermediate between those seen in pattern A and B spectra of normal superficial or intermediate cells; on one occasion this band was almost absent. The peaks at 1,080 cm^{-1} and 1,155 cm^{-1} were not shifted significantly. A few dysplastic cells showed increased amplitude of the 1,244 cm^{-1} band compared with pattern A spectra.

The spectra of malignant cells (either squamous or endocervical) resembled pattern B of normal squamous superficial and intermediate cells. Compared with pattern A spectra of normal cells, there was significant reduction of the amplitude of the 1,026 cm^{-1}, 1,080 cm^{-1}, and 1,155 cm^{-1} bands; increased amplitude of the 1,244 cm^{-1} band; and significant shifts of the peaks of the 1,080 cm^{-1} and 1,150 cm^{-1} bands to about 1,085 cm^{-1} and 1,165 cm^{-1}, respectively. These spectral changes were the same for both squamous cell carcinoma and adenocarcinoma of the cervix.

The spectra of koilocytes followed a pattern similar to pattern B and were virtually identical to those of dysplastic cells with greatly diminished glycogen band at 1,026 cm^{-1}. Anucleated cells, seen in the malignant cervical smears, displayed spectra similar to pattern B or, less often, pattern A.

FT-IR Microspectroscopy of Cytologically Normal Cells of Normal, Dysplastic, or Malignant Cervical Samples. We assessed the spectra of cytologically normal cells from the cervical smears of 10 normal women, 7 women with cervical dysplasia, and 5 women with cervical cancer. From each smear, we obtained the spectra of about 100 randomly chosen cells. These spectra were evaluated by classical spectroscopy (frequency of spectral patterns, position of important peaks, and peak intensity ratios) and by the chemometric approach.

Frequency of spectral patterns. Over 97% of the cells were morphologically either intermediate or superficial; the rest were parakeratotic, anucleated, atypical, or koilocytes. It is reemphasized that the intermediate and superficial cells from all types of smears appeared morphologically normal.

There are wide variations in the distribution of the various spectral patterns in each group (Table 1). It is apparent, however, that in neoplastic samples, pattern A spectra are about half as frequent as in normal samples (average frequencies for normal, dysplasia, and cancer are 42.3%, 20.9%, and 29.4%, respectively). The frequency of type B spectra in neoplastic samples is correspondingly higher (average frequencies for normal, dysplasia, and cancer are 46.6%, 68.4%, and 63.8%, respectively). These differences did not reach statistical significance, except for the increased frequency of pattern B spectra in dysplastic samples compared with normal samples ($P = 0.05$, Mann–Whitney U test). The frequency of intermediate-pattern or of poor-quality spectra did not differ between groups.

Peak location. There were no statistically significant shifts in peak positions among the three groups (Table 2). Of note, the upward shift of the 1,105 cm^{-1} and 1,153 m^{-1} peaks in pattern B spectra from normal cervical samples was maintained in the spectra of cells from dysplastic or malignant samples.

Band intensity ratios. We determined four band-intensity ratios for pattern A and three for pattern B spectra (Table 3). Pattern A spectra of normal cells from normal smears differed significantly from those of normal cells from dysplastic smears. In the dysplasia group, compared with normal, the 1,080 cm^{-1}/amide II, 1,026 cm^{-1}/amide I, and 1,026 cm^{-1}/amide II ratios were significantly diminished ($P < 0.01$). In cancer samples, these ratios were diminished even further, being significantly lower than those in either normal or dysplastic samples ($P < 0.01$). This decrease in ratios (i.e., in pattern A spectra) parallels the progression of cervical carcinogenesis (normal → dysplasia → cancer). In contrast, the amide I/amide II ratio did not change in any of the three groups. In pattern B spectra, the 1,080 cm^{-1}/amide II and 1,080 cm^{-1}/amide I ratios showed no change in dysplastic samples compared with normal samples; their reduction in cancer samples compared with either normal or dysplasia was small but statistically significant. Again, the amide I/amide II ratio was statistically unchanged between groups. Individual values showed a small degree of overlap among all groups (data not shown).

Chemometric Analysis. *Pattern A spectra*. To explore differences in the pattern A spectra of normal and dysplasia smears, a calibration reference consisting of representative pattern A spectra of cytologically normal cells from normal smears and of cytologically normal cells from dysplastic smears was created. Spectra derived from such cells from cytologically normal smears were assigned a dummy variable of 0, and those selected from cytologically dysplastic smears were assigned a dummy variable of 1. A rank of 6 was selected for discrimination purposes.

All spectra of individual cells in each cervical smear belonging to the three diagnostic categories (normal, dysplasia, and cancer), were tested against this calibration, and a predicted value for each spectrum was derived. Spectra corresponding to each smear were correlated and those yielding F ratios >0.99 were excluded from further analysis. The predicted values of the remaining spectra were averaged, yielding one predicted value per smear; for example, in the normal group (consisting of 10 smears), 10 average predicted values were calculated. After this, for each diagnostic group we

Table 2. The location of IR spectroscopic peaks of normal, dysplastic, and malignant cervical samples

Peak location, cm^{-1} (mean ± SD)					
Normal ($n = 10$)		Dysplasia ($n = 7$)		Cancer ($n = 5$)	
Pattern A	Pattern B	Pattern A	Pattern B	Pattern A	Pattern B
1027.20 ± 0.84	—*	1027.50 ± 0.83	—*	1026.7 ± 0.61	—*
1080.43 ± 0.34	1079.16 ± 2.60	1079.40 ± 2.47	1078.1 ± 4.5	1080.6 ± 0.01	1078.60 ± 2.5
1105.75 ± 2.11†	1114.41 ± 4.53†	1102.5 ± 3.96†	1112.8 ± 6.0†	1102.3 ± 2.9†	1118.4 ± 5.5†
1153.38 ± 0.71	1171.70 ± 6.43	1153.83 ± 1.59	1173.9 ± 9.3	1154.10 ± 0.20	1173.8 ± 5.6
1242.25 ± 4.22	1241.63 ± 3.23	1243.43 ± 3.35	1242.4 ± 3.92	1242.05 ± 2.51	1241.63 ± 3.23
1544.01 ± 1.68	1544.51 ± 1.56	1544.00 ± 1.59	1545.2 ± 2.4	1544.9 ± 1.61	1545.2 ± 1.8
1652.38 ± 0.48	1653.58 ± 2.7	1652.1 ± 0.34	1653.58 ± 2.7	1652.1 ± 0.39	1653.4 ± 2.0

Values represent the mean ± SD of the values of each sample, obtained as in *Methods*. Statistically significant ($P < 0.001$, t-test) are the shifts of peaks at 1,105 cm^{-1} and 1,153 cm^{-1} in pattern A to higher wavenumbers in pattern B of all groups. *, peak not apparent; †, approximately 1/3 of the spectra showed this peak clearly.

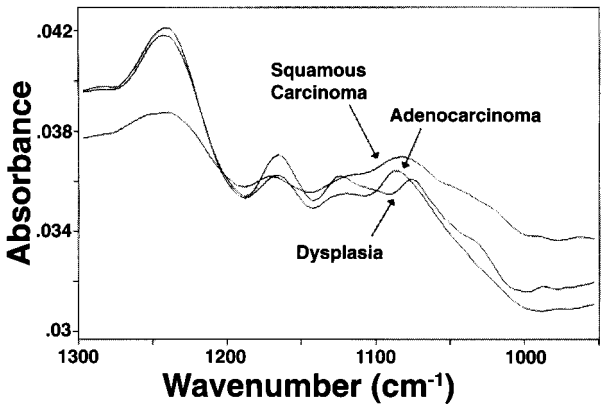

FIG. 2. FT-IR spectra of dysplastic and malignant cervical cells. Representative spectra of a dysplastic, a squamous carcinoma, and an adenocarcinoma cell (950–1,300 cm^{-1}). Their pattern is close to pattern B shown by normal squamous epithelial cells (Fig. 1).

calculated the mean and SD of these predicted values. These values (mean and SD) from each diagnostic category were fitted to normal distribution curves, yielding three separate curves: one each for normal, dysplasia, and cancer. Fitting the data to normal curves was reasonable because the individual predicted values of pattern A spectra from each diagnostic group followed a virtually normal frequency distribution.

Fig. 3*A* shows the results of this analysis. The distribution curves from the normal and cancer samples are clearly separated, with limited overlap. The curve of the dysplasia samples overlaps extensively with that of cancer samples and to some extent with that of normal samples, with its peak very close to that of the cancer curve. The average predicted values differ significantly ($P < 0.001$) between normal and dysplasia and also between normal and cancer, but not between dysplasia and cancer (Table 4).

Pattern B spectra. By using the same methodology, pattern B spectra from the cervical samples described above were analyzed (rank 5). As shown in Fig 3*C*, the curves of each diagnostic category are better separated than those of pattern A, their peaks being about equidistant from each other. Similar to pattern A, the differences between normal and dysplasia and also between normal and cancer are statistically significant ($P < 0.01$); there is no difference between dysplasia and cancer (Table 4).

In an additional chemometric analysis, the calibration curve used was based on a calibration reference consisting of representative pattern A spectra of cytologically normal cells from normal and malignant smears. Spectra derived from such cells from cytologically normal smears were assigned a dummy variable of 0, and those that were selected from cytologically malignant smears were assigned a dummy variable of 1. A rank of 9 was selected for discrimination purposes. This analysis is better suited to assess potential spectral differences between normal and malignant cervical samples directly than one using a calibration reference based on spectra from normal and dysplastic samples. Fig. 3*B*, depicting these results, indicates significant separation of the normal and cancer distribution curves; here, however, the normal and dysplasia curves have essentially coincident peaks, with total overlap of the latter on the *x* axis. In contrast to the previous analyses, in this case there is no statistically significant difference between the normal and dysplasia groups, whereas the differences between normal and cancer and also the dysplasia and cancer groups are statistically significant ($P < 0.001$). Similar analysis with the pattern B spectra (rank 6) demonstrates that the three distribution curves are distinct, with varying degrees of overlap (Fig. 3*D*). The same pattern of statistical differences between the three different groups is maintained ($P < 0.01$).

Our chemometric analysis of cervical spectra is not exhaustive; other calibration references can be used. Those presented here reflect our intention to assess spectral differences associated with the stages of cervical carcinogenesis.

Finally, we attempted to assess whether this type of analysis may aid the diagnosis of cervical neoplasia. As shown in Fig. 4, we plotted the average predicted value of the pattern A spectra of a given cervical sample versus that of the pattern B spectra of the same sample. We generated two graphs, one for each calibration reference. The values generated by using the calibration reference created from representative spectra from cytologically normal cells from either normal or dysplastic samples, are plotted in Fig. 4 (*Upper*). Those values generated by using the calibration reference created from spectra from cytologically normal cells from normal and malignant samples are plotted in Fig. 4 (*Lower*).

There is no clear separation of the three groups in either graph; instead, in both graphs there is some overlap between groups. However, there is clustering of samples belonging to the three diagnostic groups. When spectra of normal and dysplastic cells are used to create the calibration curve (Fig. 4 *Upper*), there are two clusters of points—one consisting of the normal samples and one of the neoplastic samples (dysplasia and cancer combined). When spectra of normal and malignant cells are used to create the calibration curve (Fig. 4 *Lower*), there are two different clusters of points—one consisting of the normal and dysplastic cells, and the other consisting of the malignant cells. Although the limited sample sizes preclude firm conclusions, these findings nevertheless raise the possibility that this analysis may provide a method for the diagnostic assessment of cervical samples.

Table 3. IR band intensity ratios of pattern A spectra in normal, dysplastic, and malignant cervical smears

	Ratio				
Pattern	1,080 cm^{-1}/AmII	1,026 cm^{-1}/AmI	1,026 cm^{-1}/AmII	1,080 cm^{-1}/AmI	AmII/AmI
Normal ($n = 10$)					
A	1.13 ± 0.038	0.79 ± 0.007	1.77 ± 0.129	ND	0.51 ± 0.002
B	0.15 ± 0.012	ND	ND	0.09 ± 0.006	0.57 ± 0.027
Dysplasia ($n = 7$)					
A	0.76 ± 0.015	0.59 ± 0.010	1.17 ± 0.045	ND	0.54 ± 0.002
B	0.14 ± 0.012	ND	ND	0.085 ± 0.009	0.60 ± 0.045
Cancer ($n = 5$)					
A	0.51 ± 0.016	0.43 ± 0.014	0.77 ± 0.050	ND	0.58 ± 0.001
B	0.11 ± 0.010	ND	ND	0.07 ± 0.003	0.59 ± 0.031

In each cervical sample the mean ± SD of the intensity ratios of all spectra of pattern A or B was determined. For each group, the mean ± SD of the individual means was calculated; these values were compared between groups (*t*-test). In all comparisons of cell types (normal vs. dysplasia, normal vs. cancer, and dysplasia vs. cancer), significant ($P < 0.01$) differences were seen in ratios 1,080 cm^{-1}/AmII, 1,026 cm^{-1}/AmI, and 1,026 cm^{-1}/AmII (for pattern A) and in ratios 1,080 cm^{-1}/AmII and 1,080 cm^{-1}/AmI (for pattern B). AmII, amide II; AmI, amide I; ND, not determined.

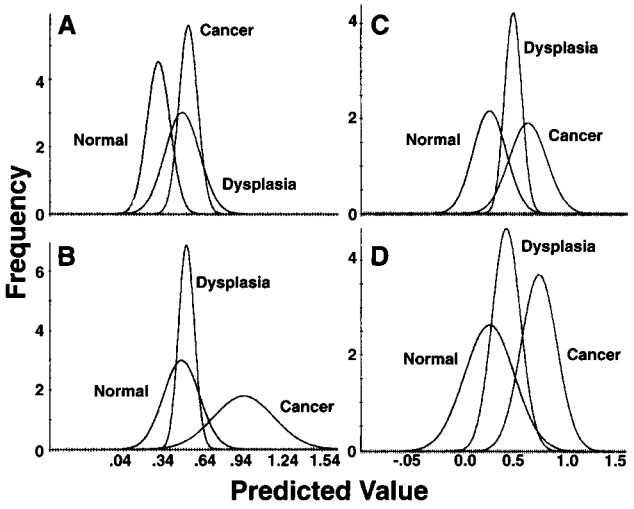

FIG. 3. Chemometric analysis of spectra of normal, dysplastic, and malignant cervical samples. Pattern A spectra: The calibration reference was created from representative spectra from cytologically normal cells from either normal and dysplastic samples (*A*) or from normal and malignant samples (*B*). Pattern B spectra: The calibration reference was created from spectra from cytologically normal cells from either normal and dysplastic samples (*C*) or from normal and malignant samples (*D*).

DISCUSSION

Our data (*i*) describe the mid-IR spectral features of various normal cervical cells as well as of dysplastic and malignant cervical cells and (*ii*) show that the spectra of cytologically normal cells from dysplastic or malignant cervical samples differ significantly from the spectra of cytologically normal cells from normal cervical samples.

Studies to date have provided the IR spectra of either cell pellets or of tissue sections. As a result, the spectral features of cell types could only be inferred. In neither type of study was a single cell (isolated from other cells) examined. In studies of cultured cell lines it was assumed that the spectrum of the cell pellet represented that of the (identical) individual cells (13). Our approach provides reproducibly high quality IR spectra of individual cells. It offers the advantage that after spectroscopy, the cell can be studied by additional means, including morphological and cytochemical assays. Thus, the spectra of the cell types commonly encountered in cervical samples have been obtained and analyzed unambiguously.

The bulk of our study includes superficial and intermediate squamous cervical cells, which constitute the overwhelming majority of exfoliated cervical cells. Analysis of the spectra of over 2,000 such cells disclosed that there is no spectral difference between superficial and intermediate cells and that both cell types normally display three distinct spectral patterns: pattern A, pattern B, and an intermediate pattern. If we exclude the poor-quality (nonanalyzable) spectra, the average frequencies of A, B, and intermediate spectra are 45%, 50%, and 5%, respectively.

Table 4. Chemometric analysis: The average predicted values of normal, dysplastic, and malignant cervical samples

	Normal - Dysplasia Calibration		Normal - Cancer Calibration	
	Pattern A	Pattern B	Pattern A	Pattern B
Normal (n = 10)	0.33 ± 0.09	0.43 ± 0.18	0.47 ± 0.13	0.26 ± 0.24
Dysplasia (n = 7)	0.51 ± 0.13	0.69 ± 0.09	0.50 ± 0.06	0.43 ± 0.14
Cancer (n = 5)	0.56 ± 0.07	0.86 ± 0.21	0.93 ± 0.22	0.75 ± 0.16

Values are given as mean ± SD. *P* values: Normal (N) - Dysplasia (D) calibration reference: Pattern A, N vs. D < 0.001, N vs. C < 0.001, D vs. C no difference; Pattern B, N vs. D < 0.01, N vs. C < 0.01, D vs. C no difference; Normal - Cancer (C) calibration reference: Pattern A, N vs. D no difference, N vs. C < 0.001, D vs. C < 0.001; Pattern B, N vs. D no difference, N vs. C < 0.01, D vs. C < 0.01.

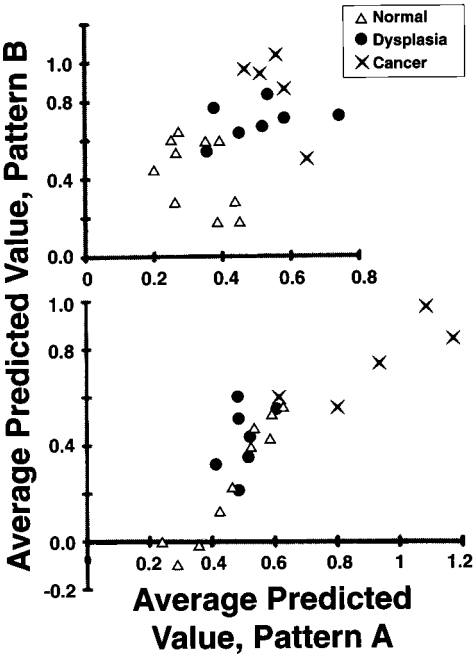

FIG. 4. Average predicted values of pattern A versus pattern B spectra of normal, dysplastic, and malignant cervical samples. The calibration reference was created from representative spectra from cytologically normal cells from either normal and dysplastic samples (*Upper*) or from normal and malignant samples (*Lower*). Although no perfect separation of normal, dysplastic, and malignant samples is achieved, clustering of samples is evident.

There are three main differences between pattern A and B spectra. Compared with pattern A, in pattern B the amplitude of the band peaking around 1,027 cm^{-1} is dramatically reduced; the 1,105 cm^{-1} and 1,153 cm^{-1} peaks are shifted toward higher wavenumbers; and the peak intensity ratio 1,080 cm^{-1}/amide II is dramatically reduced. The chemical basis for these differences is unclear. Reduction in the amount of glycogen in cells exhibiting pattern B spectra may, at least partially, explain the reduced amplitude of the 1,027 cm^{-1} band, which is a cardinal feature of pattern B. This notion is supported by the observations that (*i*) mammalian glycogen shows spectral features similar to pattern A in the area of interest; (*ii*) as cervical cells mature from basal to parabasal, intermediate, and finally superficial cells, progressively they lose part of their glycogen content (11); and (*iii*) the amount of glycogen in the cervical cells, assessed cytochemically, correlates with these spectral patterns. Nevertheless, direct proof is required before such a conclusion is reached; this also is true of the assignment of additional peaks.

The cells of each population of superficial or intermediate cells evaluated in this study show no apparent morphological differences among themselves. That each cell type exhibits three different spectral patterns suggests significant structural heterogeneity. One can speculate that these cell subpopulations may reflect developmental steps or subgroups with distinct functions.

The spectra of the remaining types of cervical cells are based on a limited number of observations. It appears, however, that a pattern similar (or identical) to pattern B is the only or the predominant pattern displayed by parabasal, endocervical, koilocytic, dysplastic, and malignant cells. Anucleated cells produced either pattern A or pattern B spectra. More data need to be gathered on these cells.

The second area of emphasis of our study was the comparison of the spectra of the cytologically normal superficial and intermediate squamous cells among the three groups (normal, dysplasia, and cancer), each defined by conventional clinical

and cytological criteria. These groups reflect the known stages of cervical carcinogenesis. Their spectra were compared by using both a classical approach and the chemometric method.

Following the classical approach, we assessed pattern frequencies, peak locations, and band intensity ratios. The difference in frequency with which each pattern occurred was not statistically significant between groups. Nevertheless, there was a clear trend for the neoplastic samples to have more pattern B spectra, with a consequent reduction in pattern A and intermediate spectra. There was no difference in peak position when spectra of the same pattern were compared. Band intensity ratios showed significant differences between the three groups. These differences have four features. First, they concern both spectral pattern A and pattern B, being more pronounced in the former. Second, in pattern A spectra these changes are pronounced in magnitude; for example, in cancer, the 1,026 cm^{-1}/amide II ratio is less than half of that in the normal group. Third, these ratios decrease progressively from normal → dysplasia → cancer, paralleling the evolution of cervical carcinogenesis. For example, the average 1,026 cm^{-1}/amide II ratio is in the normal group is 1.77, in dysplasia 1.17, and in cancer 0.77. Finally, individual values overlap between groups, no doubt reflecting the continuity of the carcinogenic process.

The classical assessment indicates significant differences in the spectra of cytologically normal cells from dysplastic and malignant cervical samples compared with those from normal samples. In contrast, the chemometric analysis, which examines even subtle spectral differences of the entire spectral segment under consideration, has provided a more thorough and comprehensive assessment of the spectral differences between the three groups. Both pattern A and pattern B spectra differ significantly among the three groups, although there is some overlap between them. Indeed, there is a continuum of changes from normalcy to malignancy, suggesting that a continuously evolving process is operative during cervical carcinogenesis.

As our data reiterate, in this type of analysis the calibration reference affects, to some extent, the outcome. For example, when the calibration reference is based on normal and dysplastic samples, the separation between the normal and dysplastic groups is greater when we use a calibration reference based on normal and malignant samples. However, regardless of the calibration reference used, the cancer group is always separated from the normal group. This observation underscores the magnitude of the differences between the two extremes of normalcy and malignancy in the human cervix as well as the power of the spectroscopic study.

This study has important implications. It suggests that when the neoplastic process, defined morphologically, is developed in the cervix, the normal-*appearing* cells surrounding those that are morphologically abnormal have extensive (and measurable) structural changes. We do not yet have sufficient data on the spectral features of neoplastic cells to assess how similar their spectra are to those of the surrounding normal-appearing cells. Nevertheless, the key point here is that in our study of over 2,000 individual superficial and intermediate cervical cells that all look alike under the microscope, those from neoplastic samples (compared with those from normal samples) have significant structural, chemical, or metabolic alterations detected by IR microscopy; concordant results were obtained with both the classical and the chemometric analysis. Quantitatively, these changes cover a continuum that parallels the transition from entirely normal to dysplasia and then to malignancy. The inference, therefore, is that whatever their nature, these changes either are involved in or are a product of cervical carcinogenesis. In either case, one may surmise that cellular changes associated with the neoplastic process may occur earlier than presently recognized, involving cells that by current morphological methods are characterized as normal. These changes indicate a strong trend and one may be able to use this information for classification purposes.

The significance of the morphologically normal but spectroscopically abnormal cells is unclear. They may represent an early stage of neoplasia not recognizable morphologically or a "milder neoplasia" compared with that involving the overtly abnormal cells. One may hypothesize that this change is correlated with various stages of activity of the human papilloma virus that is frequently associated with cervical neoplasia (15).

Further work will be required to clarify whether these cells, for example, define an earlier stage of neoplasia, an accessory to the diagnosis of cervical neoplasias, or a target for preventive or therapeutic interventions. Of interest, we already have identified a clinical correlate of IR spectroscopic abnormalities in cervical cells. Women with history of dysplasia, who at the time of the spectroscopic evaluation had cytologically normal smears, displayed abnormal IR spectra (unpublished data). Thus, this approach may prove useful in the study of cervical diseases in general.

Our findings may explain the observation that pellets of neoplastic samples in which the dysplastic or malignant cells are far fewer than 5% of the total generate such grossly abnormal spectra. It is possible that the abnormal spectra of neoplastic cervical samples examined as cell pellets result, at least to some extent, from spectral abnormalities of the normal-appearing cells and not solely from abnormalities of the (few) neoplastic cells.

Another implication of our observations concerns their diagnostic value. This approach, though laborious and preliminary, may have some diagnostic value; the limited number of subjects evaluated precludes any confident conclusion. It is worth noting that if this method proves diagnostically useful, it will shift the emphasis when "reading the Pap smear" from the abnormal-appearing to the normal-appearing cells. As the latter far outnumber the former, this may diminish the possibility of a missed diagnosis.

In conclusion, our work establishes an approach to obtain high quality IR spectra from individual cells; describes the spectral features of many normal and (in a limited way) of most abnormal cervical cells, suggesting extensive structural heterogeneity among the superficial and intermediate cervical cells; indicates that the normal-appearing intermediate and superficial cells of the cervix from women with neoplasia are structurally different from the corresponding cells of normal women; and indicates that hitherto-unrecognized structural changes may be involved in or accompany cervical neoplasia.

1. Rigas, B., Morgelo, S., Goldman, I. S. & Wong, P. T. T. (1990) *Proc. Natl. Acad. Sci. USA* **87,** 8140–8144.
2. Wong, P. T. T., Goldstein, S. M., Grekin, R. C., Godwin, T. A., Pivik, C. & Rigas, B. (1993) *Cancer Res.* **53,** 762–765.
3. Wong, P. T. T., Wong, R. K., Caputo, T. A., Godwin, T. A. & Rigas, B. (1991) *Proc. Natl. Acad. Sci. USA* **88,** 10988–10992.
4. Morris, B. J., Lee, C., Nightingale, B. N., Molodysky, E., Morris, L. J., Appio, R., Sternhell, S., Cardona, M., Mackerras, S. & Irwin, L. M. (1995) *Gynecol. Oncol.* **56,** 245–249.
5. Wood, B. R., Quinn, M. A., Burden, F. R. & McNaughton, D. (1996) *Biospectroscopy* **2,** 143–153.
6. Cohenford, M., Godwin, T. A., Cahn, F., Bhandari, P., Caputo, T. A. & Rigas, B. (1997) *Gynecol. Oncol.* **66,** 59–65.
7. Fung, M. F. K., Senterman, M., Eid, P., Faught, W., Mikhael, N. Z. & Wong, P. T. T. (1997) *Gynecol. Oncol.* **66,** 10–15.
8. Zhengfang, G. E., Brown, C. W. & Kisner, H. J. (1995) *Appl. Spectrosc.* **49,** 432–436.
9. Haaland, D. M. & Thomas, E. V. (1988) *Anal. Chem.* **60,** 1193–1201.
10. Haaland, D. M. & Thomas, E. V. (1988) *Anal. Chem.* **60,** 1202–1208.
11. Koss, L. G. (1992) *Diagnostic Cytology and its Histopathology* (Lipincott, Philadelphia), 4th Ed.
12. Wong, P. T. T., Papavassiliou, E. D. & Rigas, B. (1991) *Appl. Spectrosc.* **45,** 1563–1567.
13. Rigas, B. & Wong, P. T. T. (1992) *Cancer Res.* **52,** 84–88.
14. Villa, L. L. (1997) *Adv. Cancer Res.* **71,** 231–241.